The mechanism of transition in the wake of a thin flat plate placed parallel to a uniform flow

By HIROSHI SATO AND KYOICHI KURIKI
Aeronautical Research Institute, University of Tokyo, Japan

(Received 10 February 1961)

A study was made of the laminar-turbulent transition of a wake behind a thin flat plate which was placed parallel to a uniform flow at subsonic speeds. Experimental results on the nature of the velocity fluctuations have made it possible to classify the transition region into three subregions: the linear region, the non-linear region and the three-dimensional region.

In the linear region there is found a sinusoidal velocity fluctuation which is antisymmetrical with respect to the centre-line of the wake. The frequency of fluctuation is proportional to the $\frac{3}{2}$ power of the free-stream velocity, and the amplitude increases exponentially in the direction of flow. The behaviour of small disturbances in the linear region was investigated in detail by inducing velocity fluctuation with an external excitation—actually sound from a loud-speaker. Solutions of the equation of a small disturbance superposed on the laminar flow were obtained numerically and compared with the experimental results. The agreement between the two was satisfactory.

When the amplitude of fluctuation exceeds a certain value, the growth rate deviates from being exponential due to non-linear effects. Although velocity fluctuations in the non-linear region are still sinusoidal and two-dimensional, the experimental results on the distributions of amplitude and phase indicate that the flow pattern may be described by the model of a double row of vortices. This configuration lasts until three-dimensional distortion takes place in the final subregion, the three-dimensional region, in which the fluctuation loses regularity and gradually develops into turbulence without being accompanied by abrupt breakdown or turbulent bursts.

1. Introduction

The laminar-turbulent transition of boundary layers is a well-known phenomenon which has been investigated theoretically and experimentally since the beginning of this century. The detailed process of transition, however, still remains unclarified. In the initial period of investigation, interest lay mainly in determining the transition Reynolds number, which was important from the practical viewpoint. Modern developments in experimental techniques of flow measurement have made it possible to make detailed observations of velocity fluctuations in the boundary layer. Thus, investigations in the last decade have been focused on the understanding of the mechanism of transition. Recent

experimental results have indicated that two typical patterns of velocity fluctuation are essential in the transition. One is the regular sinusoidal fluctuation of small amplitude, and the other is the instantaneous turbulent burst of much higher intensity.

Sinusoidal fluctuations were first discovered experimentally by Schubauer & Skramstad (1948) in the boundary layer along a flat plate. They obtained good agreement between their results and the linearized stability theory which had been developed by Tollmien, Schlichting and others. Since then, extended studies have been made on the properties of sinusoidal fluctuations both experimentally and theoretically. Sinusoidal velocity fluctuations have been found in various flow fields at subsonic and supersonic speeds, and agreement between linearized theory and the experimental results is satisfactory (Sato 1959*a*, *b*; Laufer & Vrebalovich 1960). It is now well established that the behaviour of fluctuations of small amplitude in the boundary layer is described by the linearized theory. On the other hand, our knowledge on the turbulent burst is poor. Experimental results obtained by various investigators sometimes show disagreements, and no concrete conclusions have been obtained on the origin and the law of development of a burst. Moreover, in the transition region of free boundary layers, no bursts have been observed so far (Sato 1959*a*, *b*). In order to obtain a full understanding of the detailed mechanism of transition, more extensive studies are wanted.

The present investigation has been undertaken with the intention of clarifying the process of transition in wakes. A thin flat plate was placed in a uniform flow with zero angle of attack so as to produce a simple, well-defined wake. It is obvious that the wake of a cylinder is inadequate for detailed studies of transition since the flow field behind a cylinder is much too complicated owing to boundary-layer separation and rolling up of vortices in the wake. The velocity profile of a laminar wake was calculated by Goldstein (1933), and stability calculations based on the Orr–Sommerfeld equation were carried out by Hollingdale (1940) and McKoen (1956) in the case of large Reynolds number. It was Hollingdale (1940) who made the first systematic observation of velocity fluctuations in the wake of a flat plate by taking pictures in a water tank. Taneda (1958) has extended these observations to a wider range of Reynolds number with an improved experimental arrangement. He has found sinusoidal velocity fluctuations whose frequency is proportional to $\frac{3}{2}$ power of the flow speed. The present work was started in order to make a more detailed survey of velocity fluctuations in wakes, using modern techniques of hot-wire anemometry in a low-turbulence wind-tunnel. The first part of this paper gives a general view of the transition phenomenon. The second part deals with the sinusoidal velocity fluctuations, and the third and fourth parts are devoted to clarifying the role of non-linear effects and three-dimensional distortion in the process of development into turbulence.

2. Experimental arrangement

The experiment was conducted in a 60×60 cm low-turbulence wind-tunnel which was newly constructed at the Aeronautical Research Institute. The tunnel is of non-return type with the test-section downstream of the fan. The contraction ratio, i.e. the ratio of cross-sectional area of the settling chamber to that of the test-section, is 16:1. Eleven damping screens were installed in the settling chamber. These arrangements, incorporated with a proper design of air-intake, fan and diffuser, diminished the turbulence level at the test-section to 0·05 % at a flow velocity of 10 m/sec. Background noise and mechanical vibrations were carefully reduced by suitable construction, since they have a great influence on the transition process. The wind speed at the test-section was

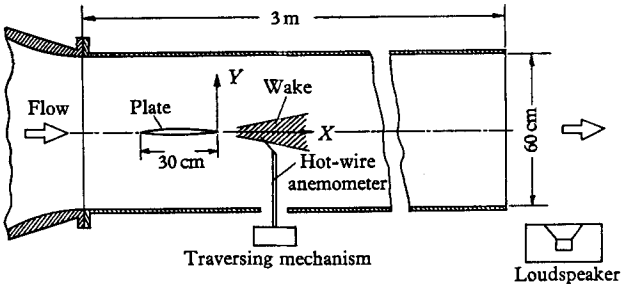

FIGURE 1. Layout of test-section.

variable from 1 to 30 m/sec. The general layout of the test-section is shown in figure 1, in which X is the distance downstream from the trailing edge of the plate, Y is measured perpendicular to the plate, and Z is the spanwise distance from the central point of the trailing edge.

The side walls of the test-section were made of aluminum plates which were adjusted in order to keep the streamwise static-pressure distribution constant. One of the side walls had slits parallel and normal to the flow which allowed the insertion and traversing of hot-wire anemometers and pressure probes in the X-, Y- and Z-directions.

The two-dimensional wake was realized behind a thin flat plate which was spanned vertically along the centre-line of the wind-tunnel. The parallel alignment between the plate and the direction of flow was accomplished by measuring the mean-velocity distribution at the trailing edge of the plate. Three kinds of flat plate were used in order to clarify the effect of the thickness of the plate, as well as the sharpness of trailing edge, on the transition process. Dimensions of these plates are summarized in table 1.

The chord and span of all plates were 30 and 60 cm, respectively. Plate I was made of aluminium, carefully machined into a thin airfoil over the whole length and polished to a mirror-like surface. Plate II was a thin brass foil without machining. Plate III was made of aluminium and was sharpened at the leading edge, with the remaining part kept at the same thickness until the square trailing edge. The Reynolds number based on the length of plate ranged from 6×10^4 to 4×10^5.

For the measurement of the mean-velocity distribution, both fine Pitot tubes and hot-wire anemometers were used, although the measurements by Pitot tubes formed a very small part of the present experiment. For the hot-wire anemometers, use was made of 10 % rhodium-platinum wire, 5 μ in diameter and about 2 mm in length. For the measurement of the w-component of velocity, the hot-wire was rotated around the axis of support.

	Maximum thickness (mm)	Thickness ratio (%)	Thickness at the trailing edge (mm)
Plate I	3	1	0·1
Plate II	0·3	0·1	0·3
Plate III	3	1	3

TABLE 1. Dimensions of plate.

The mean velocity and the root-mean-square of the fluctuating velocity were measured by conventional hot-wire equipment which has been previously reported (Sato, Kobashi, Iuchi, Yamamoto & Onda 1954). The spectral distribution of the velocity fluctuation was observed by a band-pass filter. The mean-cube of the fluctuation was measured by a newly constructed unit in which the cubic curve was approximated by the superposition of the plate currents of ten triodes which were properly biased and loaded. A mean-square output meter was constructed on the same principle. This type of circuit had the advantages of higher input impedance and lower power consumption compared with similar circuits constructed by diodes. The fluctuation patterns were observed and recorded by a dual-beam cathode-ray oscilloscope.

The anemometers were traversed in the X-, Y- and Z-directions. The X- and Z-positions were determined by scales, and the Y-position was indicated by a precision dial gauge. The accuracy of positioning was 0·2 mm in the X- and Z-directions, and 0·01 mm in the Y-direction.

The flow was artificially excited by the sound radiated from a 10 W loud-speaker placed at the exit of the test-section as shown in figure 1. The maximum available intensity of the sound was about 100 db, although a much weaker sound was enough to induce transition in the laminar wake. The excitation frequency was varied from 500 to 1000 c/s, excluding the resonance frequency of the wind-tunnel, which was about 200 c/s. The intensity of sound was uniform throughout the test-section, and no resonance effect was detected in the above-mentioned frequency range.

3. General aspects of transition

At first, measurements were made in the boundary layer along the surface of the plate. The streamwise static-pressure variation along the surface was very small because the plates were very thin. The boundary layer was laminar everywhere on the plate, and no traces of a velocity fluctuation were found even at the

highest wind-speed. The velocity profile was of Blasius-type, and the streamwise development of the boundary layer was in good agreement with the well known theoretical calculation for a flat plate. These results were quite satisfactory as regards fixing the initial condition of the laminar two-dimensional wake.

After separation at the trailing edge, the boundary layers from both sides coalesced and formed a wake, which still remained laminar to some distance downstream. The velocity profile gradually changed from Blasius-type into laminar-wake type. Velocity distributions at various X-stations are shown in figure 2, where U_0 denotes the free-stream velocity. At $X = 0$, the distribution is of Blasius-type. Until $X = 30$ or 40 mm, the distribution varies slowly, while a sharp increase of central velocity is found from $X = 40$ to 60 mm. In the figure two unusual facts are demonstrated. First the velocity at the outer part of the wake sometimes exceeds the free-stream velocity (for example, at $X = 120$ mm, $Y = 4$ to 5 mm). Secondly, the central velocity is approximately equal at $X = 60$, 120 and 150 mm.

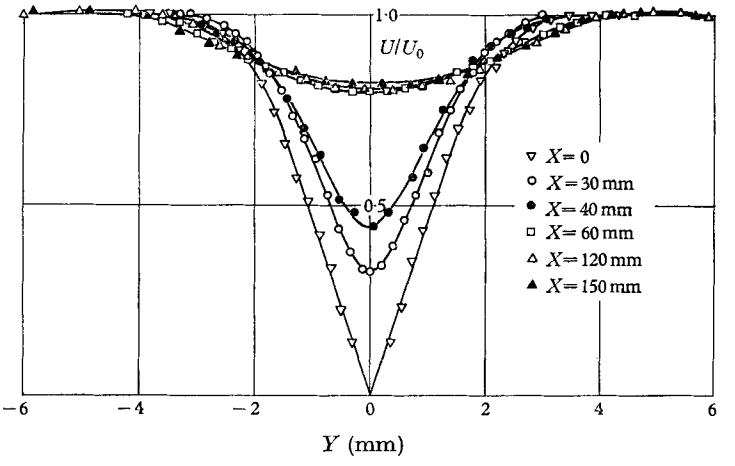

FIGURE 2. Mean-velocity distribution. Plate I, $U_0 = 10{\cdot}0$ m/sec.

In order to illustrate the streamwise variation of velocity distribution more clearly, the velocity U_c on the centre-line is plotted against X in figure 3. Curves for various experimental conditions show the same trend. The theoretical curve for the laminar wake given by Goldstein (1933) is in agreement with the experimental results when X is small. As X is increased, the experimental curves deviate from Goldstein's result, reach maxima, decrease and again increase gradually. The point of deviation from the theoretical curve may be called the 'transition point'. It must be kept in mind, however, that the transition never takes place at a point and, moreover, that the definition of transition itself is arbitrary. A more detailed account of the velocity distribution in the transition region will be given in the following paragraphs.

At $X = 5$ to 30 mm, depending on experimental conditions, there appears a velocity fluctuation whose wave-form is regular and sinusoidal. By careful investigation it was confirmed that the observed sinusoidal fluctuation was not

the result of either mechanical vibrations of the hot-wire or of acoustical resonance in the wind-tunnel. The frequency of fluctuation was the same throughout the whole region in which the wave-form was sinusoidal. The amplitude increased downstream until the wave-form was distorted into an irregular pattern. Since similar sinusoidal fluctuations have been already found in separated layers (Sato 1956, 1959*b*) and jets (Wehrmann & Wille 1958; Sato 1959*a*), the existence of sinusoidal fluctuations in the wake is not surprising. It has also been pointed out that the frequency of such fluctuations is proportional to the $\frac{3}{2}$ power of the flow velocity according to dimensional reasoning

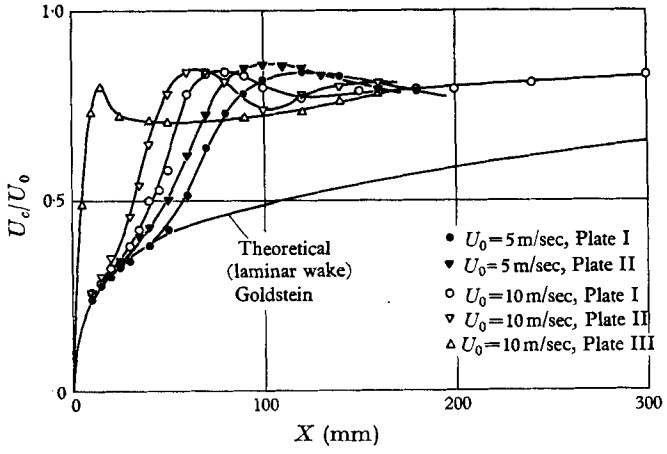

FIGURE 3. Streamwise variation of mean velocity U_c on the centre-line under various experimental conditions.

(Sato 1956). The logarithmic plot of frequency in the wake verified the same power law, as is shown in figure 4. The difference in frequency for three different plates was due to the difference in the thickness of the trailing edge. For a thick trailing edge, such as on Plate III, the thickness of the wake is comparatively large, and therefore the frequency of fluctuation is lower.

The development of the velocity fluctuations is illustrated in figures 5 and 6, which show results obtained with slight artificial excitation at the 'natural' frequency (i.e. the frequency of the sinusoidal fluctuations observed in the natural transition). Since the excitation was very slight, it had little effect on the transition process. On the other hand, the excitation improved the reproducibility of the flow field, and it was also used as a phase standard in the measurement of the phase relation of the velocity fluctuations. A detailed discussion concerning the interrelation between natural and excited transition is given in § 7. The wave-form of the u-fluctuation (figure 5) shows a gradual development from sinusoidal into irregular patterns. No turbulent bursts or momentary breakdowns have been observed. This type of transition is in contrast to that of a boundary layer on a solid wall, and is in accordance with transitions in separated layers and jets. Figure 6 is a map of fluctuation patterns at various X- and Y-positions. The sinusoidal fluctuation was observed from $X = 20$ to about 400 mm. Near the centre-line the second-harmonic component

prevailed as shown in figure 5. The irregular fluctuation first appeared near the centre-line and spread, as X was increased, until about $X = 400$ mm, where the whole wake was covered by irregular fluctuations.

It is worth while to note that at low Reynolds numbers the velocity fluctuation decays by viscous dissipation before the wave-form becomes irregular. In this case, no turbulent region exists in the wake even though the intensity of sinusoidal fluctuation may be considerable. This is another sharp contrast to the transition of a boundary layer on a solid wall, in which the continuous energy supply due to Reynolds stresses and velocity gradient is maintained. In the low

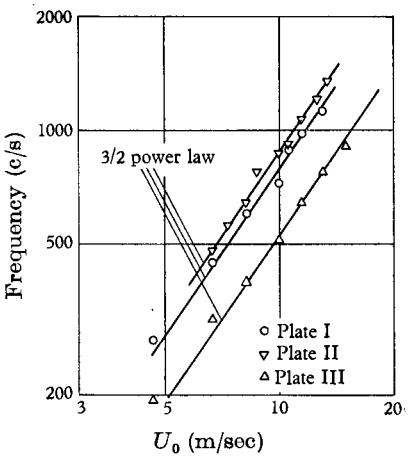

FIGURE 4. Frequency of natural sinusoidal fluctuations plotted against free-stream velocity U_0.

Reynolds number wake, the velocity gradient as well as the Reynolds stresses becomes progressively smaller downstream, and the viscous dissipation becomes pronounced. At higher Reynolds number, the wave-form of the fluctuations becomes irregular before it dies out, but it is still doubtful whether the wake becomes 'fully turbulent' or not. Moreover, even when the central part of the wake becomes turbulent, the regular fluctuation can persist in the outer part, as shown in figure 6. In these cases the definition of transition is vague. If the existence of a fully-turbulent region is a prerequisite of transition, there occurs no transition in the above-mentioned cases. Nevertheless, a high-level regular fluctuation exists in the wake and the mean-velocity distribution is different from that of laminar wake. We might call the region which is neither laminar nor turbulent the 'transition region'. In so far as we use the term 'transition' in this sense, the transition point might be the end point of the laminar region and not the beginning point of turbulent region.

The intensity of the u-fluctuations, with Plate I and $U_0 = 10{\cdot}0$ m/sec, is plotted in figure 7. When X was small, the distribution was almost similar, and positions of peak values approximately coincided with positions of maximum gradient in the mean-velocity distribution. As X was increased, the intensity increased until about $X = 60$ mm and then decreased. Distributions from $X = 60$ to 150 mm have maxima on the centre-line. This is due to the increase

of the second-harmonic component, which is shown in figures 5 and 6. The intensity of fluctuation in the present experiment was rather small compared with that in the wake behind a cylinder. This fact might be explained by the

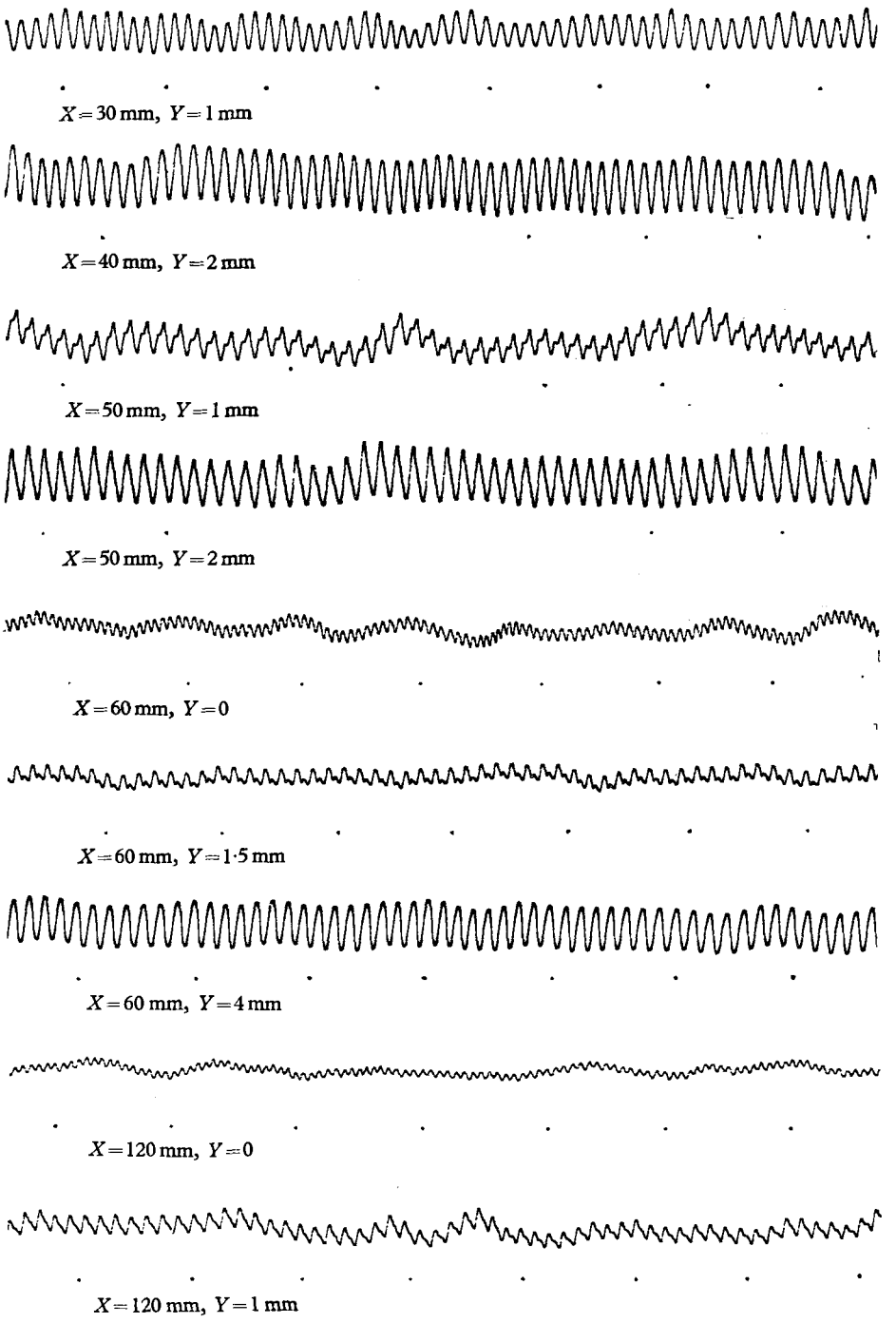

FIGURE 5. For legend see facing page.

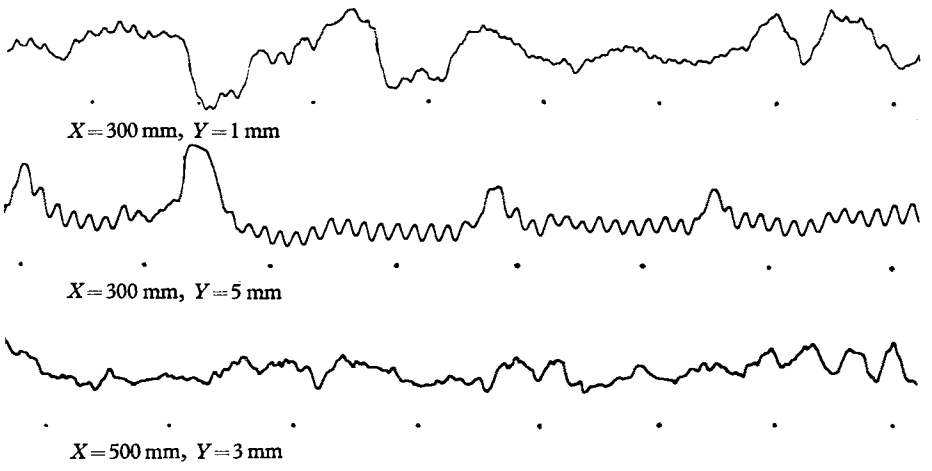

FIGURE 5. Oscillographic records of u-fluctuations in wake. Plate I, $U_0 = 10{\cdot}0$ m/sec. Time goes from left to right and time interval between dots is 0·01 sec.

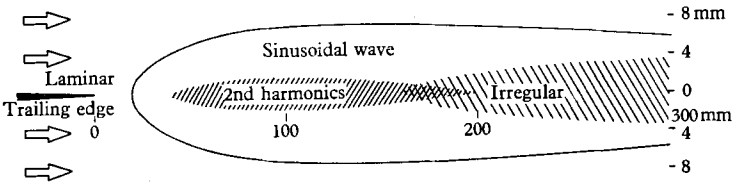

FIGURE 6. Map of fluctuation patterns. Plate I, $U_0 = 10{\cdot}0$ m/sec.

disturbance at the trailing edge of a flat plate being smaller than that behind a cylinder.

After these investigations were made on the velocity fluctuation in the transition region, we found it convenient to consider a division into three sub-regions, i.e. the linear region, the non-linear region, and the three-dimensional region, which are characterized by the pattern of fluctuations.

1. *Linear region.* In this region were observed two-dimensional sinusoidal velocity fluctuations which were amplified exponentially downstream. Referring to the previous investigations on free boundary layers (Sato 1959*a*, *b*), it is expected that these sinusoidal fluctuations may be described by the linearized theory. This region ends at the X-station where the amplitude of fluctuation reaches the 'linearity limit': in other words, where the law of amplification deviates from being exponential. The mean-velocity distribution in this region is in agreement with Goldstein's theoretical result.

2. *Non-linear region.* As a result of amplification of the sinusoidal fluctuations, second and higher harmonics are found in the wave-form, as shown in figure 5. Two-dimensionality is still maintained, that is, $\overline{w}^2$ is small compared with $\overline{u}^2$ and $\overline{v}^2$ and the phase difference of the velocity fluctuations in the Z-direction is small. The variation of mean velocity is remarkable in this region, being the result of intense energy supply from the mean flow to the velocity fluctuations.

3. *Three-dimensional region.* Further downstream the velocity fluctuation becomes three-dimensional, while some periodicity still persists. The wave-form

is irregular in the central part and is sinusoidal at the outer part of the wake. The turbulent region starts where the remaining regularity diminishes.

In the following paragraphs the mechanism of transition will be made clearer by describing in detail these three regions.

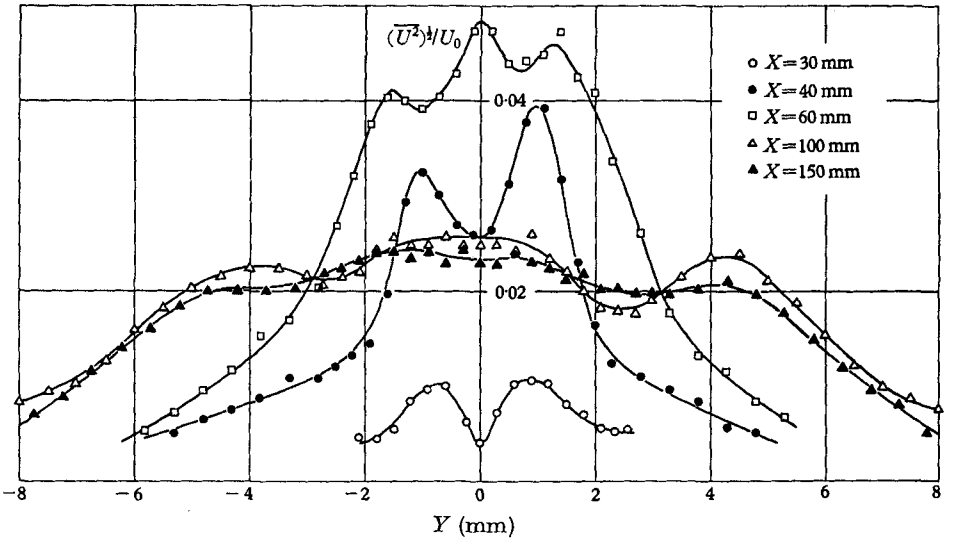

FIGURE 7. Distribution of intensity of u-fluctuations. Plate I, U_0 = 10·0 m/sec.

4. The linear region

As shown in the previous paragraph, sinusoidal fluctuations are found in the transition region of the wake. They are weak at first, grow as the distance downstream is increased, and finally develop into irregular fluctuations still further downstream. The nature of the sinusoidal fluctuations has been clarified by both experimental and theoretical investigations.

4.1. *Experimental results*

Experiments on sinusoidal fluctuations have been made in two cases, one for natural transition and the other for transition caused by the external artificial disturbance. The latter is important for the experimental verification of linearized theory, which in turn is useful for clarifying the mechanism of the linear region in natural transition. Since natural transition results from the development of small unknown and uncontrollable disturbances, there is no essential difference between the natural and excited transition except the nature of the original disturbances. However, before detailed measurements are made with artificial excitations, it should be ascertained that the flow field is not changed too much by them. If the intensity of the artificial disturbance is too high, non-linear effects set in at X-stations that would lie in the linear region of natural transition. On the other hand, if the incoming sound is too weak, the induced fluctuation is masked by natural fluctuations, and in this case accurate measurements are difficult. The proper level of exciting sound was carefully decided as a compromise between these two considerations.

Experiments were carried out using Plate I at $U_0 = 10{\cdot}0$ m/sec. The frequency of natural fluctuations in this case was around 730 c/s. The frequency range of the artificial excitation was from 480 to 850 c/s. Outside this range the observed fluctuation was hardly affected by the sound.

The phase of the sinusoidal fluctuations was not constant in the X-direction, that is, the fluctuation was in fact a travelling wave. The propagation velocity was measured by moving a hot-wire anemometer in the X-direction. Since the

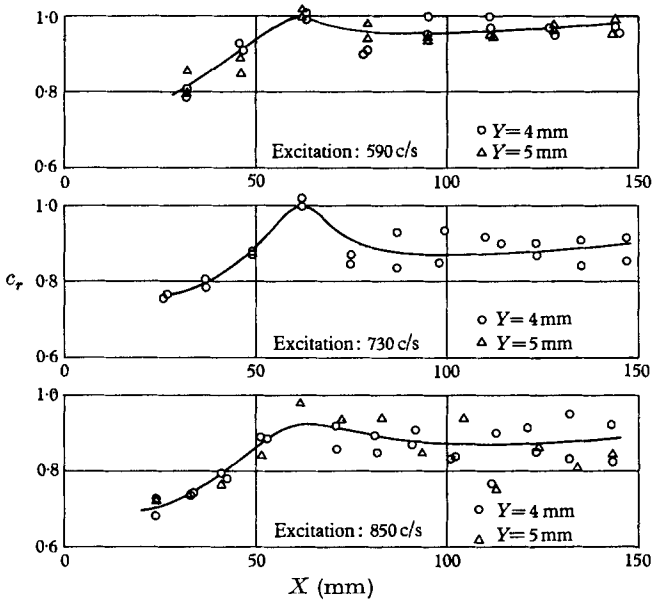

FIGURE 8. Propagation velocity of sinusoidal waves induced by artificial excitation. Plate I, $U_0 = 10{\cdot}0$ m/sec.

variation of phase in the Y-direction was remarkably large near the centre-line, as shown later, the phase difference in the X-direction had to be determined at large Y. Results for various frequencies of excitation are shown in figure 8, in which the propagation velocity c_r, expressed as a fraction of U_0, is plotted against X. The value of c_r increases as X is increased, reaches a maximum at about $X = 60$ to 70 mm, and settles at about 0·9 for larger X. It is interesting to note that the variation of c_r in the X-direction is similar to that of U_c. Detailed discussion of the values of c_r is found in §4.3.

The increase in amplitude of the spectral components in the X-direction is illustrated in figure 9, in which $(\overline{u_f^2})^{\frac{1}{2}}_{\max}$ is the maximum value of the Y-distribution, of root-mean-square intensity of the spectral component at each X-station in the presence of excitation, whose frequency was as indicated. The value was obtained by adjusting the central frequency of a band-pass filter to be exactly equal to the frequency of the sound excitation, and then traversing the hot-wire in the Y-direction. Since $(\overline{u_f^2})^{\frac{1}{2}}_{\max}$ is plotted on an arbitrary scale, comparison between values at different frequencies would be meaningless, although the relative values for the same frequency are correctly expressed. Each spectral

component was amplified exponentially at small X and deviated from the exponential form at $X = 30$ to 35 mm due to non-linear effects. From the gradient of each curve the rate of amplification in the X-direction is calculated.

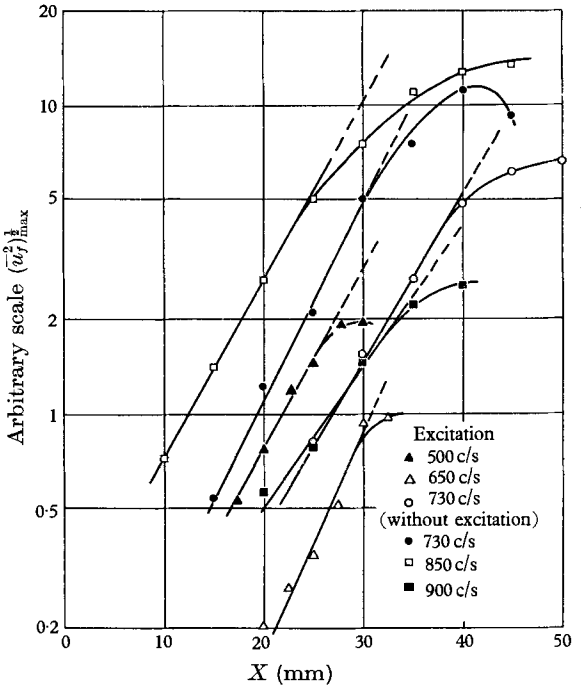

FIGURE 9. Growth of spectral components. Plate I, $U_0 = 10{\cdot}0$ m/sec.

Distributions in the Y-direction of amplitude and phase of natural sinusoidal fluctuations are shown in figure 10. The amplitude distribution has two peaks at about $Y = \pm 1$ mm, and becomes nearly zero on the centre-line. A change in phase is observed at -3 mm $< Y < 3$ mm. This is the reason why the variation of phase in the X-direction had to be measured at $Y = 4$ or 5 mm. Although a phase shift of about 70 degrees existed between $Y = -1$ and -5 mm, the phase difference at any two symmetrical points with respect to the centre-line was always approximately 180 degrees. These results are to be compared presently with the linearized theory.

Figure 11 shows distributions of amplitude and phase of the second-harmonic component (1460 c/s) which is found predominantly near the centre-line, as described before. The amplitude is a maximum at $Y = 0$, and the phase distribution shows that this component is symmetrical with respect to the centre-line. For the generation of the harmonic component the non-linear effect might be responsible. A full discussion of this point is given in the following sections.

4.2. *Theoretical considerations*

A theoretical investigation of the stability of wakes to small disturbances has been carried out by Hollingdale (1940) and McKoen (1956). Their work is restricted to the case of neutrally stable disturbances and, moreover, their

methods of approximation are rather crude. Therefore, in order to compare the foregoing experimental results with theory, calculations extending to the non-neutral case have been made with improved accuracy. Only the case of infinite Reynolds number has been considered.

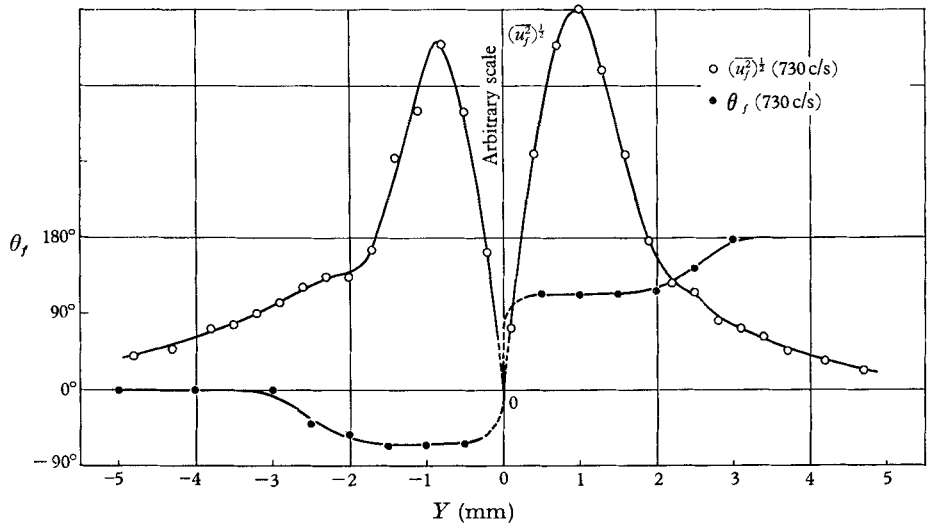

FIGURE 10. Amplitude and phase distributions of fundamental component. Plate I, $U_0 = 10{\cdot}0$ m/sec, $X = 40$ mm.

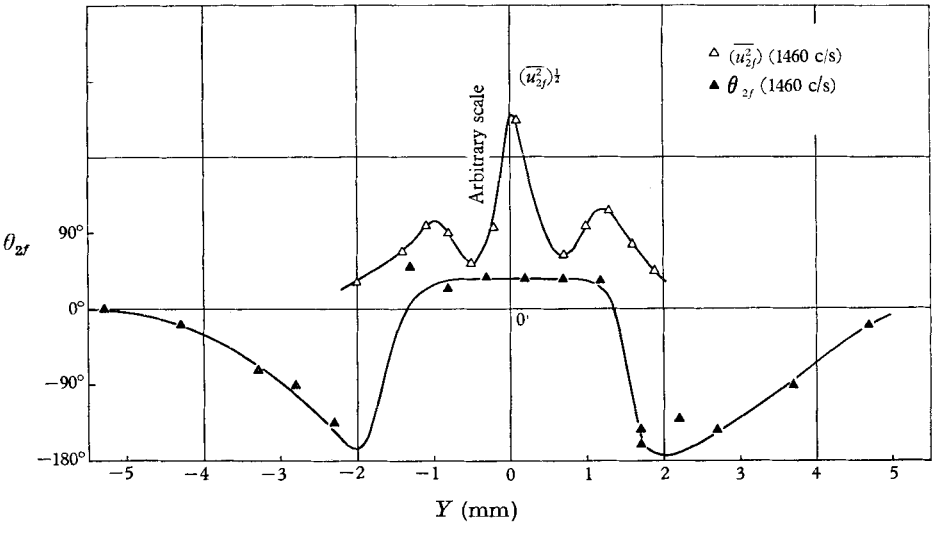

FIGURE 11. Amplitude and phase distributions of second-harmonic component. Plate I, $U_0 = 10{\cdot}0$ m/sec, $X = 40$ mm.

We follow the procedure of conventional linearized stability calculations. The basic flow is assumed to be two-dimensional and a function of y only, and lateral disturbance velocities are neglected. The disturbance velocities u and v are assumed to be functions of x, y and time t. Quantities in the equations of

motion and continuity are made non-dimensional by taking as units of velocity and length the free-stream velocity U_0 and the half-breadth b of the mean-velocity distribution. If X, Y, Z and T are the dimensional coordinates and time, the corresponding dimensionless quantities are written $x = X/b$, $y = Y/b$, $z = Z/b$ and $t = TU_0/b$.

We define a stream-function ψ such that the velocity perturbations are given by

$$u = \frac{\partial \psi}{\partial y}, \quad v = -\frac{\partial \psi}{\partial x},$$

and we assume that u and v are small enough to justify linearization of the equations of motion. We further assume that the Reynolds number is large enough for the viscous terms in the equations of motion to be neglected. (The justification for this is based on the fact that the stability characteristics of free boundary layers become insensitive to viscous effects when the Reynolds number is fairly high.) Then, assuming ψ to take the form

$$\psi = \phi(y) \exp [i\alpha(x-ct)], \tag{1}$$

in which α is the wave-number and $c = c_r + ic_i$, where c_r is the propagation velocity and c_i a measure of the rate of amplification of the disturbance, we find that ϕ satisfies the equation

$$\left(\frac{U}{U_0} - c\right)(\phi'' - \alpha^2\phi) - \frac{U''}{U_0}\phi = 0, \tag{2}$$

which is the 'inviscid' form of the well-known Orr–Sommerfeld equation.

The boundary conditions are

$$\left.\begin{aligned} \phi(0) = 1, \quad \phi'(0) = 0, \\ \phi'(\pm\infty) + \alpha\phi(\pm\infty) = 0, \end{aligned}\right\} \tag{3}$$

and the mean velocity distribution is assumed to be

$$\frac{U}{U_0} = 1 - \frac{U_0 - U_c}{U_0} \exp(-ay^2),$$

in which a is taken as 0·69315 so as to make $(U_0 - U)/(U_0 - U_c) = \frac{1}{2}$ at $y = \pm 1$. The validity of this expression is indicated in figure 13. Since, in a wake, symmetrical disturbances are more stable than antisymmetrical ones, calculations have been made only for the latter.

In order to find a set of eigenvalues which satisfies the boundary conditions, numerical integrations have been repeated by a high-speed electronic computer. The computed results for the eigenvalues α and c, taking $(U_0 - U_c)/U_0 = 0{\cdot}692$, are shown in figure 12.

Before we compare these theoretical results with experiment, we have to make a transformation of time axis and X-axis according to the relation $x = c_r t$, since the flow in a wind-tunnel is stationary and the disturbance is amplified as it travels in the X-direction. Therefore the spatial rate of amplification $\alpha c_i/c_r$ must be used instead of αc_i for the comparison with experimental results.

4.3. *Comparison of experimental results with linearized theory*

A non-dimensional plot of the velocity defect in the linear region of the wake is shown in figure 13. The theoretical distribution for a fully developed laminar wake is in the form exp $(-ay^2)$, which is indicated by a solid line. The velocity distribution at $X = 30$ mm according to the calculation by Goldstein (1933) is

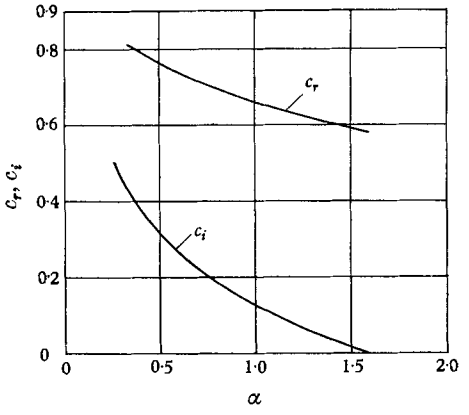

FIGURE 12. Theoretical rate of amplification and propagation velocity.

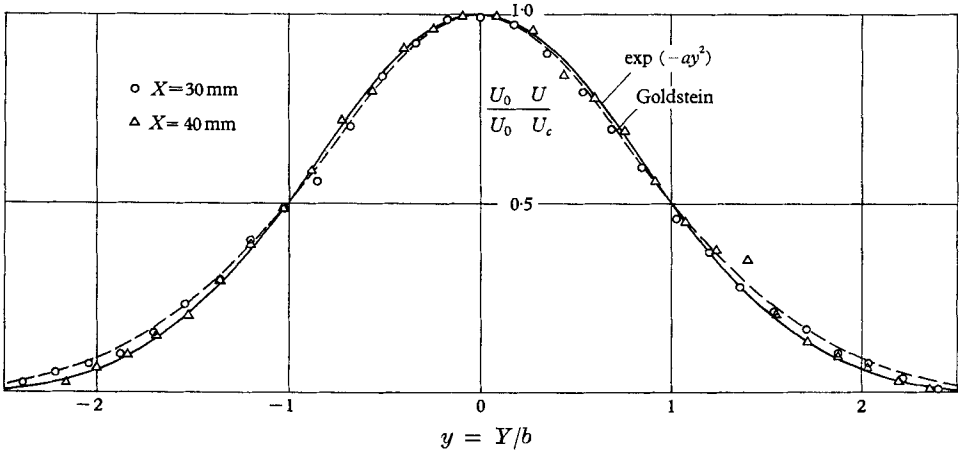

FIGURE 13. Non-dimensional mean-velocity distribution in linear region.

as shown by a broken line. The two theoretical curves are very close, and the experimental data are in good agreement with these curves. Since the distribution given by the broken line has no simple analytical expression, the exponential distribution is preferable as a basic flow for the calculation of disturbance properties.

The non-dimensional frequency αc_r of the observed natural fluctuations is plotted against Reynolds number in figure 14. Since the theoretical value of αc_r for neutral oscillations at infinite Reynolds number is 0·92, the frequency of the natural fluctuations can be assumed to lie inside the unstable zone of the

theoretical stability diagram, although the curve of neutral stability for finite Reynolds numbers has not been derived. To the right of the figure is shown the theoretical spatial amplification rate at infinite Reynolds number, which has a maximum at about $\alpha c_r = 0{\cdot}5$. Thus it is confirmed that the frequency of the sinusoidal fluctuations found in natural transition approximately corresponds to the frequency of the small disturbance which receives maximum spatial amplification according to the linearized theory.

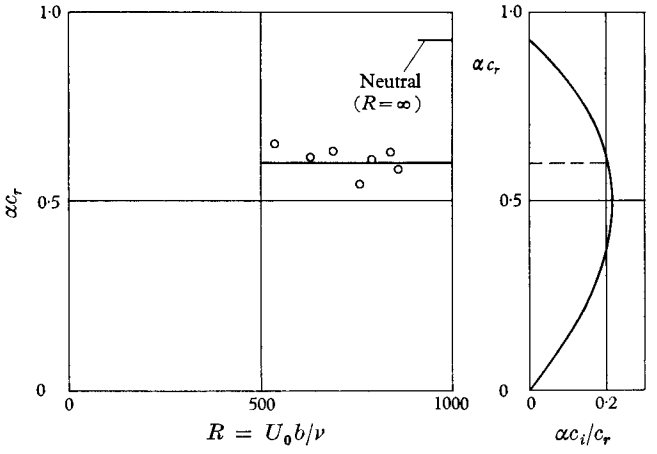

FIGURE 14. Comparison of theoretical and experimental results. Frequency of velocity fluctuation, $\alpha c_r = 2\pi f b/U_0$.

When sound waves were used as artificial excitation, it was impossible to observe the damping of disturbances just beyond the critical condition since the induced velocity fluctuations were not sufficiently strong. Therefore the neutral point was determined experimentally by the method introduced in a previous paper (Sato 1959*b*). The ratio of the intensities of spectral components with and without excitation is plotted against non-dimensional frequency in figure 15. The neutral frequency is determined as the point where the ratio becomes unity. Arrows on the abscissa indicate the theoretical values which have been obtained by various investigators: e.g. by Hollingdale (1940) who obtained two values with different methods of approximation, and by McKoen (1956). The present value of αc_r determined by numerical integration is the smallest among the four given values. The experimental results obtained under four different conditions are fairly consistent, and they agree most closely with the present theoretical estimate.

Figure 16 shows the propagation velocity and spatial rate of amplification which are obtained from experimental data such as figures 8 and 9. The solid lines are theoretical results for amplified disturbances at infinite Reynolds number. The agreement between theory and experiment is fairly good in both c_r and $\alpha c_i/c_r$.

Distributions of amplitude and phase in Y-direction are compared in figure 17. Experimental points denote the root-mean-square values of spectral components of the u-fluctuations in the natural transition, taking the maximum value as

unity and, for the phase angle of the spectral components, taking the value at $Y = -5$ mm as zero. Theoretical results are given for amplified disturbances for which $\phi(y)$ is complex. The amplitude function and phase angle for the u-fluctuations were calculated from the real and imaginary parts of $\phi'(y)$. As shown by a solid line in the figure, a gradual phase shift in the y-direction exists for the

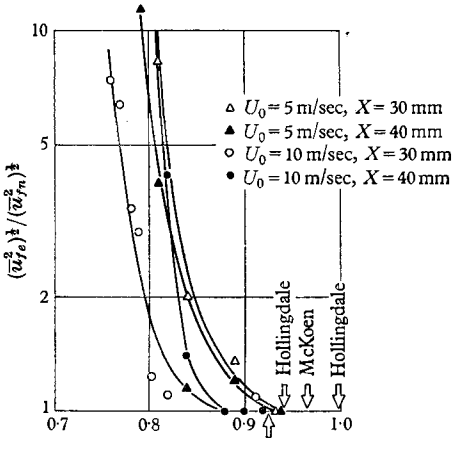

FIGURE 15

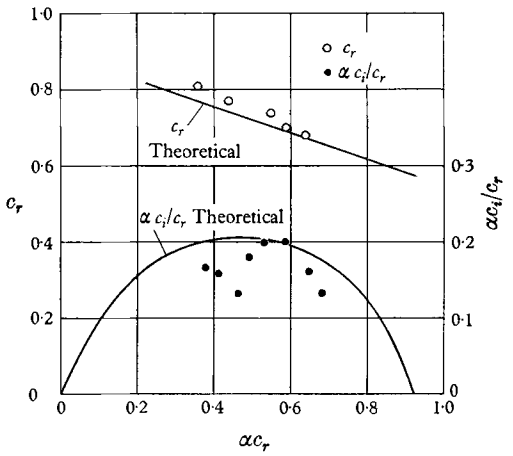

FIGURE 16

FIGURE 15. Determination of frequency of neutral oscillation. Plate I. $(\overline{u_{fe}^2})^{\frac{1}{2}}$ and $(\overline{u_{fn}^2})^{\frac{1}{2}}$ denote root-mean-square values of spectral components of frequency f with and without artificial excitation respectively.

FIGURE 16. Propagation velocity c_r and spatial rate of amplification $\alpha c_i/c_r$.

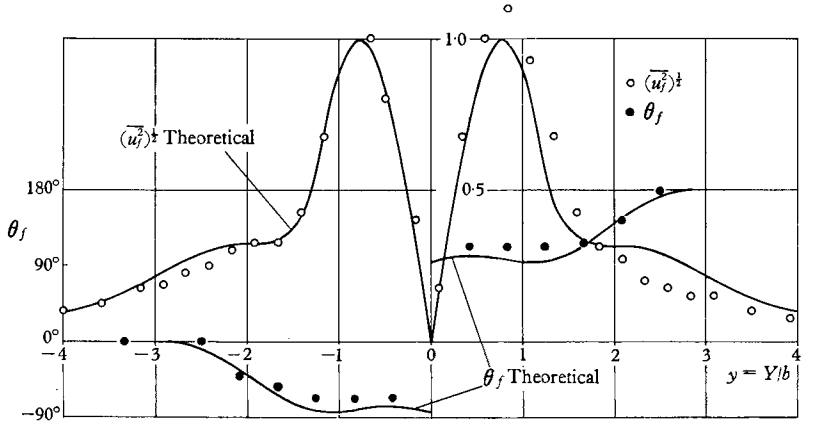

FIGURE 17. Amplitude function. In theoretical results, $\alpha = 0{\cdot}832$ and $c_i = 0{\cdot}168$.

amplified disturbance, in contrast to the case of neutral disturbances. Theoretical eigenvalues in the present case are $\alpha = 0{\cdot}832$, $c_i = 0{\cdot}168$, $c_r = 0{\cdot}692$, which correspond to a disturbance with approximately the maximum spatial rate of amplification. The agreement between theory and experiment is excellent.

Thus the experimental results on the properties of sinusoidal fluctuations in the linear region are properly described by the linearized theory. Considering

the previous results on the separated layer and jet, it is now obvious that in the transition region of a free boundary layer there exists a linear region in which sinusoidal fluctuations grow as predicted by the theory of the Orr–Sommerfeld equation.

5. The non-linear region

The upstream boundary of the non-linear region is the X-station where the growth rate of velocity fluctuations deviates from being exponential. This deviation demonstrates the role of non-linear terms in the equation of motion. This initial point of the non-linear region might be called the 'transition point' since the non-linearity is an essential feature of turbulent motion. On the other hand, the transition point defined as the end-point of laminar region in the preceding section is determined from, for instance, the streamwise variation of velocity on the centre-line such as is shown in figure 3. These two kinds of transition point, one defined from the velocity fluctuation and the other from the time-mean velocity, are found experimentally to be very close. This fact has been already pointed out in the case of separated layers and jets (Sato 1956, 1959*a*). From the experimental results it has been confirmed that the two-dimensionality of the fluctuations is still maintained in the non-linear region. The downstream boundary of the non-linear region is defined as the X-station where the fluctuations become three-dimensional so that, for instance, $\overline{u}^2$ and $\overline{w}^2$ become comparable. With Plate I and $U_0 = 10{\cdot}0$ m/sec, the extent of the non-linear region was found to be about $X = 40$ to 150 mm.

5.1. *Non-linear development of sinusoidal fluctuations*

As shown in figure 5, the non-linear effect on the wave-form of the fluctuations is observed in the vicinity of the centre-line as an increase of low-frequency irregular fluctuations. In the outer part of the wake the sinusoidal fluctuation persists with the same frequency. The non-linear effect seems to be slight between $X = 40$ and 150 mm as far as the wave-form is concerned. However, remarkable changes take place in the distributions of amplitude and phase of the spectral components, as is shown in figures 18 and 19. In figure 18, the root-mean-square values of the spectral component at the fundamental frequency are plotted on an arbitrary scale, while the relative values at various X-stations are correctly expressed. The distribution changes in a rather peculiar way as X is increased. From $X = 40$ to 80 mm, the variation is gradual. The positions of the two peaks move outwards, maintaining a roughly similar type of distribution. At $X = 120$ and 150 mm, the distribution shows three minima, at $Y = 0$ and $Y = \pm 2{\cdot}5$ mm. Referring to figure 19, we see that a 180-degree phase reversal takes place at these three points. At each X-station, 180-degree reversal is observed at $Y = 0$, except at $X = 80$ mm which is in some sense a dividing line. Now it seems possible to classify the non-linear region into two parts. The upstream part more or less resembles the linear region, although the exponential amplification of fluctuations is no longer observed. In the downstream part, the distribution functions of amplitude and phase are completely different from

those in the upstream part. It is obvious that in the non-linear region a new equilibrium is established at about $X = 100$ mm.

The next step of the investigation is to clarify the nature of the harmonic components in the non-linear region. An increase of harmonic components is expected as a result of non-linear interaction. In figure 20, the distribution of second harmonics is shown. While a remarkable increase in $(\overline{u_{2f}^2})^{\frac{1}{2}}$ takes place

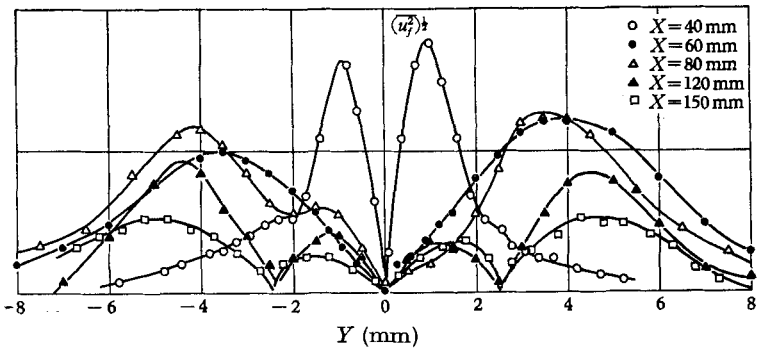

FIGURE 18. Amplitude distribution of fundamental component in non-linear region. The ordinate scale is arbitrary.

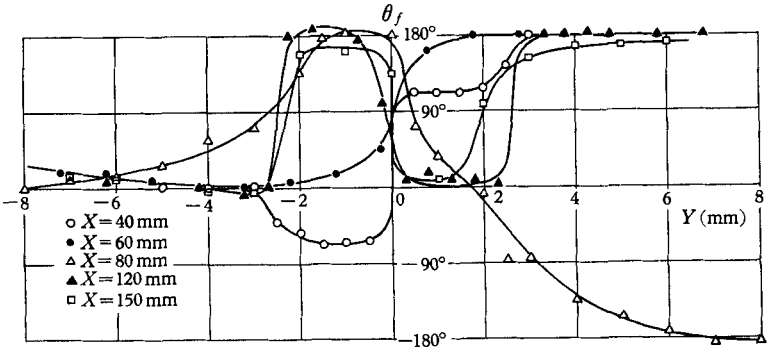

FIGURE 19. Phase distribution of fundamental component in non-linear region.

from $X = 40$ to 60 mm, it decreases downstream from $X = 60$ mm. This is a curious situation since the fundamental component still increases or only slightly decreases from $X = 60$ to 100 mm. The ratio of harmonic component to fundamental component becomes a maximum at $X = 60$ mm and decreases as X is increased further. Although non-linear effects might always be expected to increase the harmonic content, we here observe a contrary result. The distribution function of the second-harmonic component $(\overline{u_{2f}^2})^{\frac{1}{2}}$ in the Y-direction shows a reduction in the extent of the distribution from $X = 60$ to 120 mm. This fact is also unusual. A more detailed discussion of figure 20 is hardly justified, however, since the accuracy of measurement of the harmonic components was not high, owing to the unavoidable non-linearity of the characteristics of the hot-wire anemometer itself. The necessary correction for this non-linearity reached 50 % of the value of $(\overline{u_{2f}^2})^{\frac{1}{2}}$, while the harmonic component was very small compared with the fundamental component.

Another quantity which characterizes the non-linear distortion of sinusoidal fluctuations is $(\overline{u^3})^{\frac{1}{3}}$. When the wave-form remains symmetrical with respect to the zero line, the value of $(\overline{u^3})^{\frac{1}{3}}$ is zero. Thus $(\overline{u^3})^{\frac{1}{3}}$, which was determined by the use of a cubing unit, is a measure of asymmetry of the wave-form. Due to the inevitable non-linearity of the hot-wire, as mentioned before, the measured value of $(\overline{u^3})^{\frac{1}{3}}$ was not zero even for sinusoidal fluctuations when the amplitude was fairly large. Moreover, the wave-form distortion was usually accompanied by slow irregular velocity fluctuation. For these reasons, a high accuracy was not expected in the measurement of $(\overline{u^3})^{\frac{1}{3}}$. Figure 21 is the result obtained in the non-linear region. At $X = 60$ mm, the distribution is different from those at $X = 80$ and 120 mm, which again suggests the peculiar character of the region

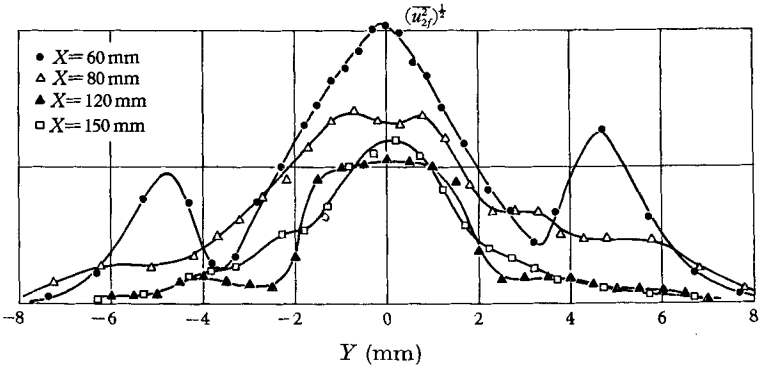

FIGURE 20. Amplitude distribution of second harmonics in the non-linear region. The ordinate scale is arbitrary.

$X = 80$ to 150 mm. It is worth while to note that in the distribution at $X = 120$ mm, the zeros of $(\overline{u^3})^{\frac{1}{3}}$ at about $Y = \pm 2$ mm coincide approximately with the phase-reversal points for the fundamental component. Outside $Y = \pm 2$ mm, the second-harmonic component is very small, so that non-linearity is manifested as the asymmetry of the wave-form. Inside $Y = \pm 2$ mm, $(\overline{u_{2f}^2})^{\frac{1}{2}}$ is nearly constant, whereas $(\overline{u^3})^{\frac{1}{3}}$ changes sign. From these facts it is expected that the generation of harmonics and asymmetrical distortion of wave-form have no simple relation, although both are undoubtedly results of non-linear interactions.

In order to clarify the situation at $X = 120$ mm, the non-dimensionalized mean-velocity distribution (figure 22) may be closely examined. We find two facts. One is the over-shoot of velocity between $y = 1{\cdot}6$ and $2{\cdot}5$, and the other is the flat distribution near the centre-line. The distribution at $X = 40$ mm is added for comparison. The peculiarity of the distribution at $X = 120$ mm is clearly seen.

5.2. *Vortex model*

The curious features of the flow field in the region $X = 40$ to 150 mm are summarized as follows:

1. Before the experiment was made, it seemed probable that in the wake the central velocity U_c increases monotonically and approaches U_0 at large X. But

at about $X = 80$ mm, U_c becomes a maximum, begins to decrease, and reaches a minimum at $X = 120$ mm before it gradually increases again.

2. The mean-velocity distribution at $X = 120$ mm is very different from that at smaller or larger X. The distribution has a flat part near the centre-line, and the velocity over-shoots the free-stream velocity at the edge of the wake.

3. The fundamental component of the velocity fluctuations at $X = 120$ to 150 mm becomes zero not only at $Y = 0$ but also at $Y \doteqdot \pm 2$ mm. The phase reversal also takes place there.

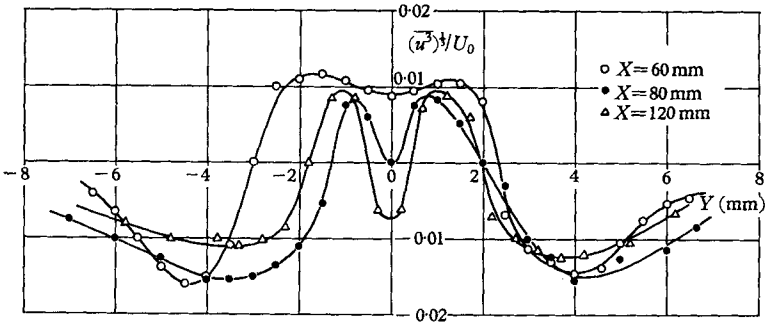

FIGURE 21. Distribution of $(\overline{u^3})^{\frac{1}{3}}$ in non-linear region.

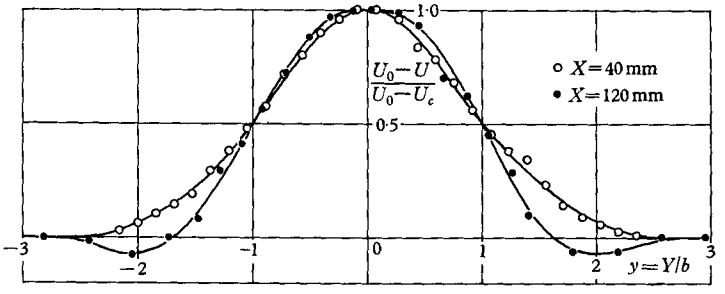

FIGURE 22. Non-dimensional mean-velocity distributions in linear and non-linear regions.

4. As X is increased, the second-harmonic component increases until $X = 60$ mm, decreases, reaches a minimum, and increases a little again as X is increased further. The distribution in the Y-direction shows a systematic change over the range $X = 40$ to 150 mm.

These features might be explained by an analytical method taking account of non-linear terms in the equation of motion. Since the linearized theory has had substantial experimental verification in the linear region, the mechanism of the non-linear region might also be clarified by an appropriate theoretical model. Practically, however, analysis of the non-linear equations of motion is very difficult, and no satisfactory theory has been reported so far. Thus we are inclined to take a tentative empirical model which explains the above-mentioned experimental facts.

In the past, many investigators have observed the formation of vortices in the wake of two-dimensional bodies, including a thin flat-plate (Hollingdale

1940; Taneda 1958). It is usually accepted that the sinusoidal fluctuations in the signal from a hot-wire anemometer corresponds to the moving vortex which is observed visually. In order to make such a correspondence apply in the present case, the physical properties posed on the vortex must be sufficiently complex to explain the wave-form of the hot-wire output. The usual simple vortex model is obviously inadequate. In order to approximate the linear region, a single row of vortices which travels in the X-direction as shown in figure 23(*a*) is useful. The adjacent vortices rotate in opposite direction and the radial distribution of circumferential velocity is assumed as shown. This model roughly explains the calculated and observed distributions of amplitude and phase of the velocity fluctuations in the linear region. The nature of the fluctuations in the non-linear region is explained as follows by the development of the single row into a double row as shown in figure 23(*b*).

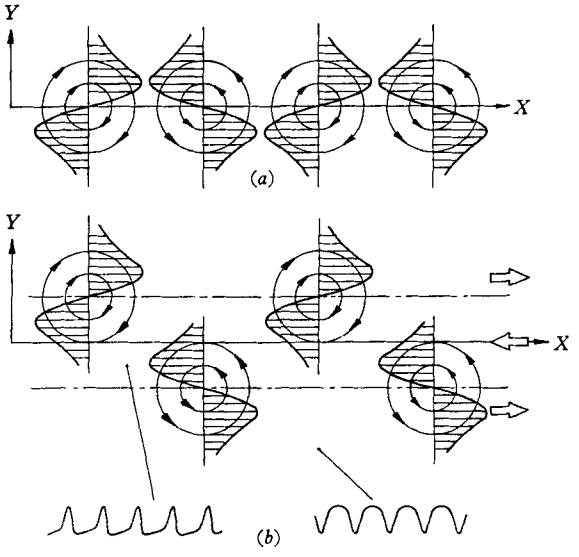

FIGURE 23. Vortex model. (*a*) Single row; (*b*) double row of vortices.

In the single row, the superposition of vortices has no effect on the mean-velocity field. On the other hand, in the double-row configuration a velocity is induced in the negative X-direction between rows of vortices, as shown by the arrow. This results in a decrease of U_c. Furthermore, a positive velocity is induced at the outer part of the wake. These facts explain the mean-velocity distribution at about $X = 120$ mm as shown in figure 22. In the double row of vortices, the phase inversion of the fundamental component takes place not only on the centre-line but on lines connecting centres of vertices in each row if the lateral spacing is large. The generation of second harmonics in the vicinity of the centre-line is also easily understood. Typical wave-forms of velocity fluctuations as expected from the vortex model are shown at the bottom of figure 23, depending on the location of hot-wire. These are in accord with the experimental observations. The change of sign of $(\overline{u^3})^{\frac{1}{3}}$ on the line connecting centres of vortices is understood from these wave-forms. Thus the process in the non-

linear region is explained by the development of the single row into a double row of vortices, and if once the double row is established, the configuration is stable and remains unchanged until three-dimensional deformation begins.

It is worth while to calculate an important geometrical parameter of a double row of vortices, that is, the ratio of lateral to longitudinal spacings. The value is 0·281 in von Kármán's analysis, whereas in the present experiment it is about 0·39. This comparatively large lateral spacing allows the phase inversion of the fundamental component on the lines connecting centres of vortices. This fact is in contrast to the case of the wake of a circular cylinder, in which the phase reversal is found only at $Y = 0$ (Roshko 1954).

5.3. *Interaction between spectral components*

In the linear region, spectral components of different frequencies are damped or amplified independently. In the non-linear region, however, two spectral components may interact with each other through the non-linear terms in the

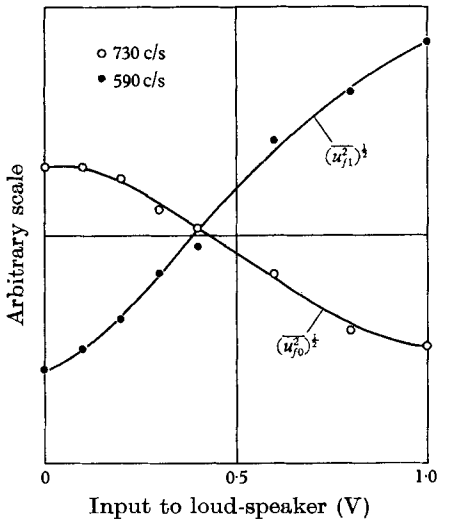

FIGURE 24. Variation of intensity of natural and excited spectral components in the non-linear region. $X = 120$ mm.

equations of motion. This interaction was experimentally investigated by superposing an artificial disturbance, that is, sound from the loudspeaker at a frequency other than that of the natural fluctuations.

At first, as the result of non-linear interaction, we expected the generation of spectral components of frequency $f_0 \pm f_1$, where f_0 and f_1 denote the frequencies of the natural and artificial disturbances respectively. However, no peaks were observed experimentally at $f_0 \pm f_1$ in the energy spectrum of the u-fluctuations. By varying the intensity of sound from the loudspeaker, the wave-form and intensity of the velocity fluctuations in the non-linear region have been investigated. Figure 24 shows the change in the root-mean-square values of two spectral components. The induced spectral component $(\overline{u_{f1}^2})^{\frac{1}{2}}$ (590 c/s) increases monotonically as the input voltage to the loudspeaker is increased. On the

other hand, the component of natural fluctuation (730 c/s) diminishes when the intensity of excitation is increased. This 'suppression effect' is more remarkable when f_1 is close to f_0. This effect means, in other words, the supply of energy from the component at f_0 to that at f_1. The detailed mechanism of the energy exchange is not yet known.

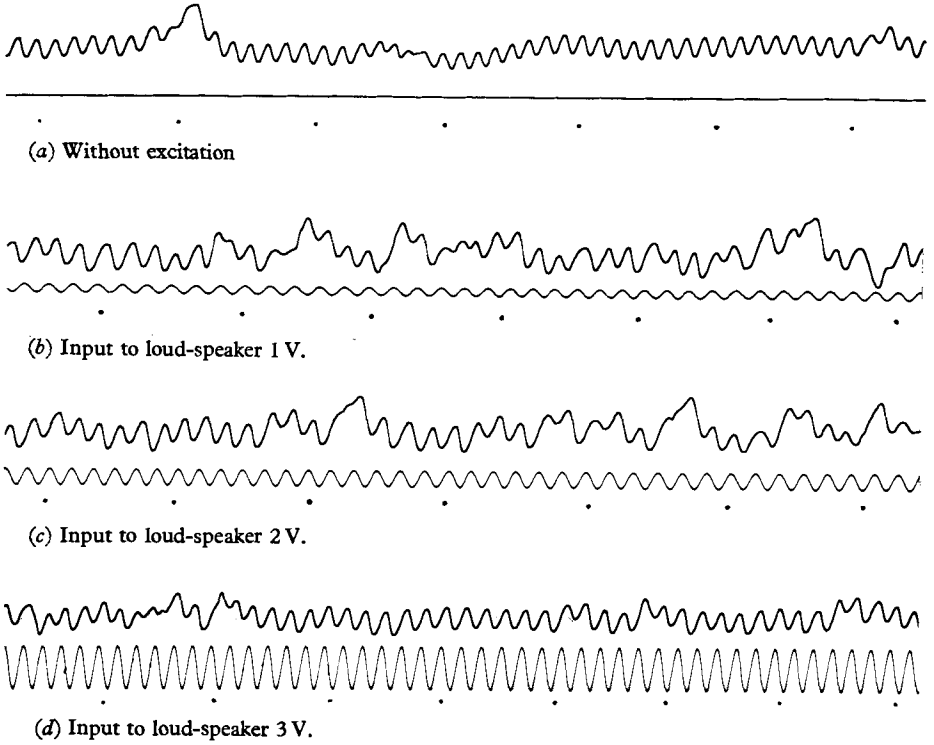

FIGURE 25. Oscillographic records of u-fluctuations in the non-linear region at $X = 120$ mm and $Y = 5$ mm. Excitation 590 c/s. Upper trace is the output from the hot-wire anemometer, and lower trace is the input to the loudspeaker. Time goes from left to right and the time interval between dots is 0·01 sec.

The wave-form in the presence of artificial excitation is shown in figure 25. Without artificial excitation the frequency of fluctuation is about 730 c/s (*a*). When the incoming sound is weak, the component of f_1 appears in a small fraction of time, while the f_0 component prevails (*b*). By increasing the intensity of sound, the probability of finding the f_1 component increases (*c*), and with the maximum intensity of sound the f_0 component is hardly found (*d*). From these records, it is obvious that the probability of finding induced fluctuation is a function of intensity of the artificial disturbance. No periodicity was found in the occasional change of the frequency of fluctuation.

6. Three-dimensional region

In the linear and non-linear regions, velocity fluctuations are approximately two-dimensional. The distortion of two-dimensional waves—in other words, the three-dimensional deformation of the row of vortices—takes place in the final

subregion of transition, the three-dimensional region, in which regularities in the fluctuations gradually diminish until the fully turbulent wake is formed. If the Reynolds number of flow is small, the fluctuation energy decays by viscous dissipation before the development into turbulence is completed. In this case, there is no turbulent region and the three-dimensional region is also hardly observed.

With the use of Plate I at $U_0 = 10{\cdot}0$ m/sec, the physical process which takes place in the three-dimensional region was as follows.

The double row of vortices formed in the non-linear region became unstable at about $X = 150$ mm. As a first sign of the deformation of the vortices, irregular wave-forms were observed near the centre-line of the wake while the fluctuation was still sinusoidal in the outer part. As X was increased, the region of irregular fluctuations extended into the outer part until the whole breadth of the wake was covered. At the same time, the phase relation of the sinusoidal fluctuations with respect to the Z-direction became irregular, and w-fluctuations became comparable in magnitude with u-fluctuation. The turbulent wake was thus established at about $X = 400$ mm, although the intensity of fluctuation was much less there compared with that in the non-linear region. No instantaneous turbulent bursts have been observed so far in this region. The change of wave-form was gradual.

Before we go into the quantitative discussion, we may suitably introduce some physical quantities to characterize the three-dimensionality. From the consideration that the difference in mean-velocity distribution at various Z-stations is small, three quantities concerning the velocity fluctuation have been used. They are the relative magnitude of $(\overline{u^2})^{\frac{1}{2}}$ and $(\overline{w^2})^{\frac{1}{2}}$, the phase relation in the Z-direction, and the distribution of spectral components at various Z-stations.

The ratio $(\overline{w^2})^{\frac{1}{2}}/(\overline{u^2})^{\frac{1}{2}}$ is plotted against Y in figure 26. At $X = 150$ mm, u- and w-fluctuations are nearly the same in magnitude, or $(\overline{w^2})^{\frac{1}{2}}$ is even greater in the region -2 mm $< Y < 2$ mm, and outside this region $(\overline{w^2})^{\frac{1}{2}}$ is very small compared with $(\overline{u^2})^{\frac{1}{2}}$. Therefore, the irregular fluctuation observed in the central region is three-dimensional, but the sinusoidal fluctuation in the outer part of the wake is still two-dimensional. At $X = 300$ mm, the ratio is close to unity over the whole breadth of the wake. This fact resulted from the faster decay of $(\overline{u^2})^{\frac{1}{2}}$ rather than the growth of $(\overline{w^2})^{\frac{1}{2}}$ in the three-dimensional region. The value of $(\overline{w^2})^{\frac{1}{2}}/(\overline{u^2})^{\frac{1}{2}}$ at $X = 300$ mm is close to that in the fully developed wake behind a cylinder.

The straightness of the front of the sinusoidal wave is expressed by the phase relation in the Z-direction at large Y. The experimental result is shown in figure 27, in which the phase angle at $Z = 0$ is taken to be zero. At small X, the variation in the Z-direction is small. This means that the wave is approximately two-dimensional and propagates in the X-direction. At larger X, a phase difference of more than 180 degrees is observed at some Z-station, while the direction of propagation as a whole still remains in the X-direction. As mentioned before, the wave-form at large X is irregular near the centre-line of the wake. This means that the double row of vortices is first distorted in the region between rows. For instance, the phase of the velocity fluctuations at $X = 250$ mm could

not be determined experimentally because of the irregularity in the central part of the wake. The phase distribution in the Z-direction at large Y might still be significant, since it expresses the three-dimensional distortion in a large scale. As shown in figure 27, the Z-station of the phase lag or advance is approximately fixed at various X-stations. This fact might have arisen from imperfections of

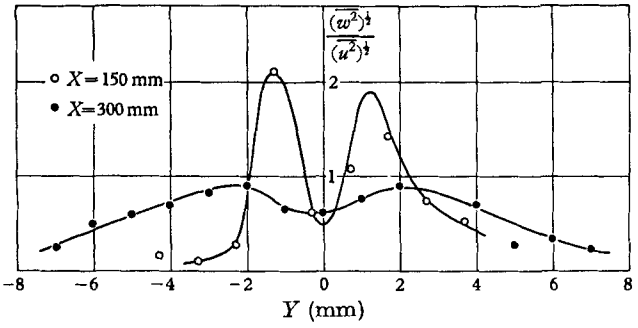

FIGURE 26. Distribution of $(\overline{w^2})^{\frac{1}{2}}/(\overline{u^2})^{\frac{1}{2}}$ at $X = 150$ and 300 mm.

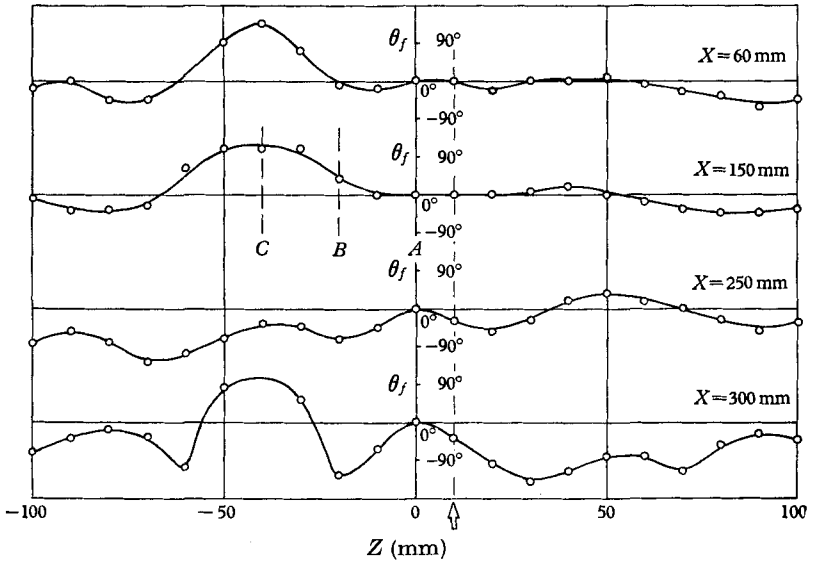

FIGURE 27. Spanwise distribution of phase of fundamental component at various X-stations in the outer part of the wake. Arrow indicates the station where detailed measurements were made.

the flat plate. Upon careful inspection of the plate, a slight waviness (about 0·2 mm in height) was found in the trailing edge at about $Z = -40$ mm. Since all measurements in the linear and non-linear regions were made at $Z = 10$ mm, as indicated by an arrow in figure 27, the experimental results described in preceding sections were uninfluenced by disturbances produced by this waviness. However, since the slightest spanwise irregularity can have a decisive effect on the breakdown of the laminar boundary layer on a solid wall (Schubauer 1958; Tani 1960), a measurement has been made on the distribution of spectral com-

ponents at three Z-stations A, B and C as denoted in figure 27. A and C are stations of maximum lag and advance respectively, and B is the midway station. The experimental results obtained at A and C are in good accordance with those at $Z = 10$ mm where all systematic measurements have been made. On the other hand, the distribution at B with $X = 150$ mm is somewhat different. The 180-degree phase shift is observed only at $Y = 0$ and the maximum value of amplitude is about 1·3 times that at $Z = 10$ mm. The phase configuration suggests the single-row configuration at B, although it is accompanied by an appreciable distortion. At $X = 200$ mm, the difference between the three Z-stations is not observed any more. From the observations made so far, the peculiar region around station B has no decisive effect on the transition process in the whole wake. This fact is in contrast to the case of transition of the boundary layer along a solid wall, which depends to an important extent on the three-dimensionality in the layer.

The three-dimensional region is succeeded by the turbulent region, on which no detailed measurements have been made in the course of the present investigation.

7. Discussion

First of all, the relation between natural and artificially excited transition must be clarified, because in the present experiment the transition was often initiated by sound from a loudspeaker. Generally speaking, in wind-tunnels there are various kinds of residual disturbance such as the free-stream turbulence, acoustic noise, mechanical vibration, etc., which undoubtedly have great influence on the transition process. These residual disturbances usually change day by day, and the reproducibility of transition pattern is sometimes very poor. And, moreover, the magnitude and nature of these disturbances are not the same for different wind-tunnels; therefore, experimental results on so-called natural transition obtained at different places are usually not comparable. We may assume that transition would take place in a similar way if levels of residual disturbances were smaller than certain limits. But even if this assumption is true, no one knows these limits, and it is probable that disturbances in existing wind-tunnels are almost always too great.

The advantages of artificial disturbances are twofold; one is to specify the nature and intensity of the predominant disturbance which induces the transition, and the other is to improve the reproducibility of the transition process. When the intensity of the artificial disturbance is considerably higher than that of residual disturbances, the reproducibility of the transition pattern is improved remarkably. However, if the intensity is too high, the pattern of transition is completely changed from that of natural transition. The frequency and amplitude of artificial disturbances are therefore to be determined by consideration of these two conditions.

A sound wave is one of the simplest and most convenient forms of artificial disturbance, since the frequency and intensity can be changed very easily. However, the excitation by sound extends uniformly over the whole flow field, and a point of excitation cannot be specified. Sometimes, the applicability is restricted by acoustical resonance of the wind-tunnel. In these respects the

vibrating ribbon (Schubauer & Skramstad 1948) is a more satisfactory measure than sound waves. But it is difficult to apply the ribbon technique to a wake and, moreover, the disturbance generated by a ribbon is undesirably large in such highly unstable flows as wakes and jets. The transition might be induced by the ribbon even when it does not vibrate, and the growth of disturbances is completed in a small region which is not suitably large compared with the dimensions of the ribbon. Although the excitation by sound is not localized, its effect is greatest at the X-station where the spatial amplification of the impressed disturbance is a maximum. As a matter of fact, the velocity amplitude of the sound may be extremely small: for instance, 0·1 cm/sec for sound at 80 db. Therefore, the induced velocity fluctuation is observable only when it is

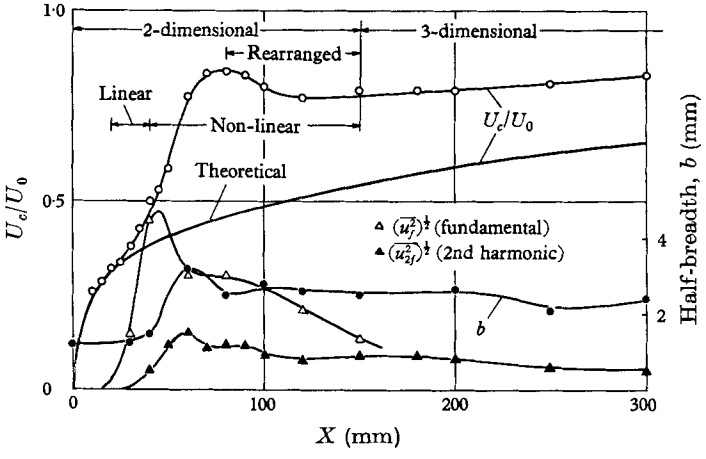

FIGURE 28. Streamwise variation of various quantities in the transition region. $U_0 = 10{\cdot}0$ m/sec, Plate I. $(\overline{u_f^2})^{\frac{1}{2}}$ is the maximum value at each X-station, and $(\overline{u_{2f}^2})^{\frac{1}{2}}$ is the value at $Y = 0$. Both are plotted on an arbitrary scale.

amplified about 100 times. Thus, it is possible to consider that the excitation is applied at an original point of amplification. The propagation velocity, rate of amplification and distribution function of spectral components in the linear region were determined in our experiments by the use of sound excitation. Wave-forms, the mean-velocity distribution and the distribution of total energy $\overline{u^2}$ were observed without sound excitation.

Some of the experimental results described in the preceding sections are summarized in figure 28, which provides a general view of the mechanism of transition. The transition region is classified into three subregions, linear, non-linear and three-dimensional. The linear region in which the sinusoidal velocity fluctuation was amplified exponentially extended from $X = 20$ to 40 mm, and this was followed by the non-linear region in which a two-dimensional double row of vortices was established as a stable configuration. The three-dimensional region started at about $X = 150$ mm and was succeeded by a turbulent region at about $X = 400$ mm. This result was found with Plate I at $U_0 = 10{\cdot}0$ m/sec, the corresponding Reynolds number based on the length of plate being $2{\cdot}1 \times 10^5$. Under different experimental conditions, the relative extent of each subregion

was, of course, different. However, the essential features of transition were concluded to be identical. In order to obtain a better understanding of the transition phenomenon, the mechanism of transition in other flow fields is now to be compared with the present result.

First, the wake of a circular cylinder is considered. Many extensive investigations have been carried out on the double row of vortices in the wake of the cylinder since the pioneering work by von Kármán. Hot-wire measurements were made by Kovásznay (1949) and Roshko (1954). Roshko has pointed out the great difference in the flow pattern behind cylinders with different Reynolds number. Therefore, before we make a comparative discussion, we have to establish the correspondence of Reynolds number between the two types of wake. It seems reasonable to compare the drags of a cylinder and flat plate in uniform flow, which are expressed by

$$D_{\text{plate}} = 1{\cdot}328\sqrt{(U_0^3 \mu \rho l)},$$
$$D_{\text{cylinder}} = C_D \tfrac{1}{2}\rho U_0^2 d,$$

in which l and d are the streamwise length of the plate and the diameter of the cylinder respectively. The boundary layer on the plate is assumed laminar everywhere. Since the drag is a measure of energy taken out of the flow, the velocity defect and velocity fluctuation might well be of the same level if the drag is equal. Thus, by putting $D_{\text{plate}} = D_{\text{cylinder}}$, we have

$$l/d = 0{\cdot}38 C_D \sqrt{R_l},$$

in which $R_l = U_0 l/\nu$. The present experimental conditions for a plate, $l = 30$ cm, $U_0 = 10{\cdot}0$ m/sec, may thus correspond to $d = 0{\cdot}18$ cm and $U_0 = 10{\cdot}0$ m/sec for a cylinder, the Reynolds number $U_0 d/\nu$ being 1200. According to the classification by Roshko, this Reynolds number belongs to the 'irregular range' in which the periodic vortex shedding is accompanied by irregular velocity fluctuations.

In the wake of a cylinder there exists no linear region in the present sense, that is, the sinusoidal fluctuation is of high intensity and always decays downstream. The mechanism of generation of vortices is different for the two types of wake. Behind a cylinder there are two separated layers from the wall, which are laminar at first and become turbulent before the rolling-up into vortices is completed at Reynolds numbers below 10^5. The continuity of the boundary layer into the wake is much smoother for the case of a flat plate. Besides these differences in the mechanism of generation, the double row of vortices in the wake of a cylinder might correspond to that in the non-linear region of the wake of a flat plate. Thus, in the wake-like velocity distribution, the anti-symmetrical two-dimensional double row of vortices is a stable configuration. The three-dimensional distortion of these vortices leads the gradual change into turbulence.

The transition of a two-dimensional jet has also been found to be characterized by sinusoidal velocity fluctuations which grow exponentially and develop gradually into turbulence (Sato 1959*b*). Observed features of the sinusoidal fluctuations were in good agreement with predictions of linearized theory. Generally speaking, the nature of transition of a jet is very close to that of a wake behind a thin plate. The separated layer from a sharp edge, though it is not a

symmetrical flow field, exhibits a similar nature of transition to jets and wakes (Sato 1959*a*). Thus, in free boundary layers including wakes, jets and separated layers, the process of transition is to a large extent similar, although in the wake behind a cylinder there is some difference, as mentioned above.

We now compare the transition of the boundary layer along a solid wall. The early work by Schubauer & Skramstad (1948) on the boundary layer along a flat plate has verified the linearized theory in the linear region of transition. Concerning the non-linear region, we can point out many essential differences between free and 'fixed' boundary layers. Modern investigations on the boundary layer along a flat plate indicate the importance of three-dimensional distortion of two-dimensional waves in the process of transition (Hama, Long & Hegarty 1957; Schubauer 1958; Tani 1960). The pre-existing three-dimensionality in the laminar layer—for instance, the spanwise variation of layer thickness—is a decisive factor in the distortion of two-dimensional waves and, therefore, in the onset of turbulence. Although the role of three-dimensionality in the transition of free boundary layers is not yet fully understood, it might be much less significant than in the case of fixed boundary layers. One of the most important features in the transition of a fixed boundary layer is the generation of turbulent bursts or, in other words, sudden breakdowns of laminar flow. It is now established that the breakdown is closely related to the complicated three-dimensional distortion of originally two-dimensional waves. The development of a small patch of turbulence has been made clear experimentally (Schubauer & Klebanoff 1956). These features of the non-linear region have no counterparts in the transition of free layers. Thus it is concluded that the linear development of sinusoidal fluctuations is verified in both free and fixed boundary layers, whereas the mechanism in the non-linear region is completely different.

The formation of a double row of vortices in the wake is a peculiar fact. As mentioned in a previous paper (Sato 1959*b*), there might be some mechanism which suppresses the deformation of vortices due to a non-linear effect. The vortex theory, such as that originated by von Kármán and modified by many other investigators, might explain some of the observed results. However, it is far from a complete explanation since it fails to describe the continuity from the linear region, or to predict wavelength, etc., in relation to the mean-velocity distribution of the wake. Thus we are inclined to think that a stability calculated for disturbances of finite amplitude is required. It is expected that the observed formation of a double row of vortices is the result of a selective action which is closely related to the initial conditions and mean-velocity distribution.

The three-dimensional distortion of two-dimensional vortices is initiated by pre-existing three-dimensionality in the flow. Recently, Benney & Lin (1960) have developed a non-linear theory and calculated second-order terms assuming a periodic variation in the Z-direction for the primary fluctuations. From the present measurements of the distributions of $\overline{u}^2$ and $\overline{w}^2$ in the Y- and Z-directions, no definite conclusion was reached concerning the validity of the theory, because the calculation was made for a different type of flow field and the assumed distribution of primary fluctuation was not realized in the present experiment.

In the wake of a thin plate, the process of three-dimensional distortion is gradual in contrast to the sudden breakdown in fixed boundary layers. In boundary layers along solid walls, there is a great difference in the equilibrium mean-velocity distribution of laminar and turbulent layers. This implies a more complicated variation of energy flow in the process of transition of fixed layers than that of free layers, in which thickening of the layer takes place without appreciable change in the shape of the mean-velocity distribution. The three-dimensional region of free layers is to be investigated in the future in more detail by determining the energy balance in the region.

8. Conclusion

The experimental and theoretical investigation of the wake developed behind a flat plate placed parallel to the uniform flow indicated the following conclusions.

1. The observed mean-velocity distribution in the laminar region of a wake is in coincidence with Goldstein's calculation.

2. At a certain Reynolds number, the transition region is classified into three subregions: (1) the linear region, (2) the non-linear region, and (3) the three-dimensional region.

3. The frequency of sinusoidal velocity fluctuations found in natural transition is proportional to the $\frac{3}{2}$ power of free-stream velocity. The fluctuations correspond to the disturbance with maximum amplification according to the linearized stability theory.

4. The sinusoidal velocity fluctuations induced by artificial excitation are amplified exponentially in the linear region when the frequency of excitation lies inside the unstable zone of the stability diagram. The observed propagation velocity, rate of amplification and amplitude function of fluctuations at various frequencies are in good agreement with the predictions of linearized theory.

5. Vortex models, a single row of vortices in the linear region and an anti-symmetrical double row in the non-linear region, are useful for explaining many of the experimental results. The double row of vortices is similar to that found in the wake of a circular cylinder.

6. In the non-linear region, an increase of intensity of the artificial excitation results not only in the increase of induced velocity fluctuation of identical frequency, but also in a decrease in the amplitude of the natural velocity fluctuations. This 'suppression effect' is remarkable when the frequency of the artificial disturbance is close to that of natural fluctuation.

7. In the three-dimensional region, the double row of vortices, which is two-dimensional in the non-linear region, is subject to three-dimensional distortion. The velocity fluctuation gradually develops into turbulence without being accompanied by sudden breakdown or turbulent bursts.

The authors appreciate the stimulating discussions occurring throughout the whole course of the investigation with members of the Boundary Layer Research Group in Japan, which is directed by Professor Itiro Tani. Thanks are extended to Mr Y. Onda and Mr O. Okubo who helped to carry out the experimental work. The research was financially supported by the Ministry of Education of Japan.

REFERENCES

BENNEY, D. J. & LIN, C. C. 1960 *Phys. Fluids*, **3**, 656.

GOLDSTEIN, S. 1933 *Proc. Roy. Soc.* A, **142**, 545.

HAMA, F. R., LONG, J. D. & HEGARTY, J. C. 1957 *J. Appl. Phys.* **28**, 388.

HOLLINGDALE, S. H. 1940 *Phil. Mag.* (7) **29**, 209.

KOVÁSZNAY, L. S. G. 1949 *Proc. Roy. Soc.* A, **198**, 174.

LAUFER, J. & VREBALOVICH, T. 1960 *J. Fluid Mech.* **9**, 257.

MCKOEN, C. H. 1956 *Aero. Res. Coun., Lond., Rep.* no. 303.

ROSHKO, A. 1954 *Nat. Adv. Comm. Aero., Wash., Rep.* no. 1191.

SATO, H. 1956 *J. Phys. Soc. Japan*, **11**, 702.

SATO, H. 1959*a* *J. Phys. Soc. Japan*, **14**, 1797.

SATO, H. 1959*b* *J. Fluid Mech.* **7**, 53.

SATO, H., KOBASHI, Y., IUCHI, M., YAMAMOTO, K. & ONDA, Y. 1954 *Rep. Inst. Sci. Tech., Univ. Tokyo*, **8**, 271.

SCHUBAUER, G. B. 1958 *Proc. Boundary Layer Symposium, Freiburg*, p. 85.

SCHUBAUER, G. B. & KLEBANOFF, P. S. 1956 *Nat. Adv. Comm. Aero., Wash., Rep.* no. 1289.

SCHUBAUER, G. B. & SKRAMSTAD, H. K. 1948 *Nat. Adv. Comm. Aero., Wash., Rep.* no. 909.

TANEDA, S. 1958 *J. Phys. Soc. Japan*, **13**, 418.

TANI, I. 1960 Paper presented at 2nd Int. Congr. Aero. Sci. Zürich (Switzerland), September.

WEHRMANN, O. & WILLE, R. 1958 *Proc. Boundary Layer Symposium, Freiburg*, p. 387.